

RSC Advances



This is an *Accepted Manuscript*, which has been through the Royal Society of Chemistry peer review process and has been accepted for publication.

Accepted Manuscripts are published online shortly after acceptance, before technical editing, formatting and proof reading. Using this free service, authors can make their results available to the community, in citable form, before we publish the edited article. This *Accepted Manuscript* will be replaced by the edited, formatted and paginated article as soon as this is available.

You can find more information about *Accepted Manuscripts* in the [Information for Authors](#).

Please note that technical editing may introduce minor changes to the text and/or graphics, which may alter content. The journal's standard [Terms & Conditions](#) and the [Ethical guidelines](#) still apply. In no event shall the Royal Society of Chemistry be held responsible for any errors or omissions in this *Accepted Manuscript* or any consequences arising from the use of any information it contains.



Journal Name

ARTICLE

Injectable hydrogels by inclusion complexation between three-armed star copolymer (mPEG-*acetal*-PCL-*acetal*-)₃ and α -cyclodextrin for pH-triggered drug delivery

Received 00th January 20xx,
Accepted 00th January 20xx

DOI: 10.1039/x0xx00000x

www.rsc.org/

Jian Hu, Mingzu Zhang, Jinlin He and Peihong Ni*

We recently reported a precise modular synthesis technique and structure-property study, in which a series of acid-cleavable star-block copolymers containing poly(ethylene glycol) monomethyl ether (mPEG) and poly(ϵ -caprolactone) (PCL) blocks linked with acid-cleavable acetal groups, abbreviated as (mPEG-*acetal*-PCL-*acetal*-)₃, were prepared and characterized. In this paper, we focus on developing the acid-cleavable star-block copolymer to an injectable hydrogel that is based on the inclusion complexes between (mPEG-*acetal*-PCL-*acetal*-)₃ and α -cyclodextrin (α -CD). The gelation times for the hydrogels were tested by a vial-tilting method, and the results indicated that these gels have a fast gelation process. Wide angle X-ray diffraction (WAXD) and differential scanning calorimetry (DSC) analyses were utilized to study the formation of a channel-type structure of a crystalline necklace-like complex induced the gelation process. Scanning electron microscope (SEM) observation results showed that three lyophilized hydrogels with different components mainly exhibited porous spongelike structure. A good structure recovery property of the supramolecular hydrogels which identified by rheological test indicates that these hydrogels have great potential application in the area of injectable hydrogels. These supramolecular hydrogels show a flowable character under a large stress, and the hydrogel systems exhibit unique structure-related reversible gel-sol transition properties at a certain stress. After remove of the high shear stress, these sol solutions started to restore their network structure immediately. Furthermore, these hydrogels are essentially elastic in response to small stresses over a frequency range that covers everyday activities such as walking and running. Doxorubicin hydrochloride (DOX-HCl), as a model drug, was encapsulated into the hydrogels, and then was released from drug-loaded hydrogels because acetal groups possess pH-triggering fracture behavior. It can be expected that this kind of injectable hydrogel have promising applications in treatment of joint disease.

Introduction

Polymeric hydrogels are three-dimensional cross-linked networks of polymer complex and can absorb > 20% of its weight of water and still maintain a distinct 3D structure. Due to their highly porous structure and close resemblance to natural extracellular matrixes, they have drawn widespread attentions and have been widely used in drug delivery, tissue engineering and cell immobilization.¹⁻⁵ As reported, the cross-linked approaches for hydrogels are mainly categorized into two strategies: "chemical cross-links" and "physical cross-links". Chemical cross-linking hydrogels are usually prepared

either by a reaction between two functional polymers or adding cross-linking agents, whereas the cross-link of physical hydrogels can be provided by noncovalent interactions, such as hydrophobic interactions,^{3,6,7} charge condensation,^{3,5,7} hydrogen bonding,^{3,8} stereocomplexation,^{3,9} or supramolecular chemistry.^{3,10-12} In general, the noncovalent interactions are weaker than chemical interactions, which result in some special mechanical properties of physical cross-linking hydrogels, such as process ability, reversible volume phase transitions or diminishing viscosity under large shear stress and time dependant restoration upon relaxation. These special properties make physical cross-linking hydrogels widely used as injectable hydrogels, which should have mechanical properties quickly built up after administration and maintain sufficient strength and stiffness over their service lifetime.^{6,13}

Injectable hydrogels, which can be easily administered during the injection procedure, provide a simple and convenient route for implantation of the hydrogel. Commonly used injectable hydrogels are mainly prepared by chemical cross-linking or sol-gel phase transition of low viscosity precursors soon after injection. These precursors are low

College of Chemistry, Chemical Engineering and Materials Science, State and Local Joint Engineering Laboratory for Novel Functional Polymeric Materials, Suzhou Key Laboratory of Macromolecular Design and Precision Synthesis, Jiangsu Key Laboratory of Advanced Functional Polymer Design and Application, Soochow University, Suzhou 215123, P. R. China Tel:+86-512-65882047; E-mail: phni@suda.edu.cn (P. H. Ni)

*Electronic Supplementary Information (ESI) available: [details of any supplementary information available should be included here]. See DOI: 10.1039/x0xx00000x

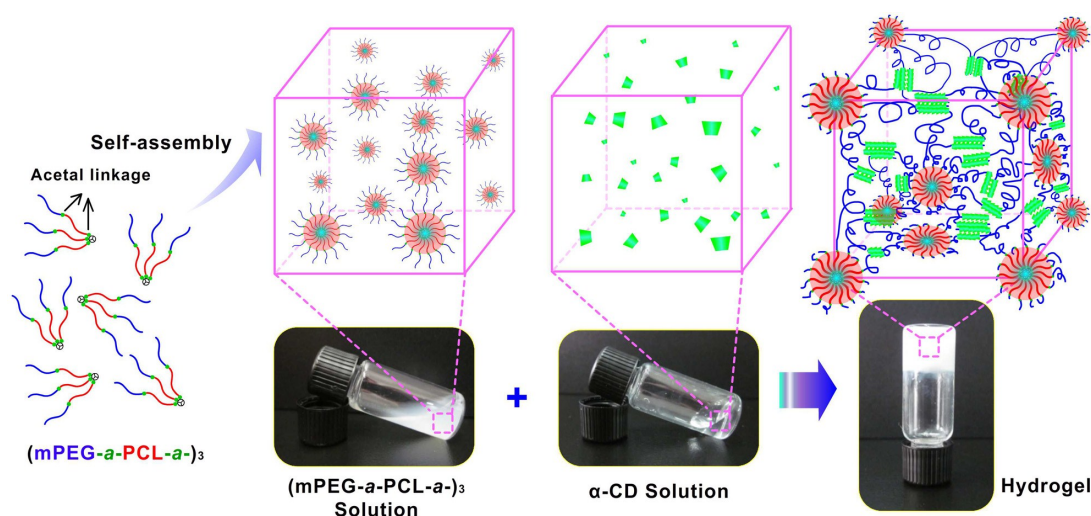
viscosity solutions before administration, but once injected, gels are rapidly formed under physiological conditions, such as body temperature, pH values and enzymes.^{1,5,7,14-17} In particular, these injectable hydrogels bring some advantages: the injectable matrix can be implanted into the human body with minimal surgical wounds, and bioactive agents or cells can be incorporated into gels simply by mixing before injection.^{6,14,18,19} Therefore, they have been widely used as controlled release depots for bioactive molecules in pharmaceutical applications.

In the past decades, supramolecular hydrogels based on the host-guest inclusion complexes between polymers and cyclodextrins (CDs) have been especially attractive as specific injectable biomaterials due to their spontaneous gelation and free of any requirement of extra treatment.²⁰⁻²² As known, the supramolecular hydrogels can be formed within a few minutes in aqueous solution after mixing the PEG-contained copolymers with α -CD.^{23,24} The inclusion complexes formed by PEG blocks and α -CD can aggregate into necklace-like crystalline polypseudorotaxanes, which can further act as physical cross-linking joints for the complex, while the uncovered hydrophilic chains function as water soluble segments. These hydrogels exhibit diminishing viscosity under large shear stress and time dependant restoration upon relaxation, which have great potential application in biomedical area, particularly as an injectable anticancer drug delivery carriers.

Controlled drug delivery devices, which can deliver and release drugs at the predetermined rates, have been used to overcome the shortcomings of conventional drug carrier systems. Considering the different pH environments at the internal and external tumor tissues (e.g. the pH value of extracellular tumors is 6.5-7.2, while it drops to a lower pH of 5.5-6.0 in endosomes and approaches pH 4.5-5.0 in lysosomes),²⁵⁻²⁷ researchers have designed some pH-responsive drug delivery devices for the controlled drug delivery systems. It will be highly beneficial to those anticancer drug delivery systems that are sensitive to the signal caused by

disease and release proper amount of drugs in response. Therefore, pH-sensitive hydrogels designed to undergo degradation in these acidic tissues should be capable of selective delivery of their therapeutic contents. In the past decades, there have been reported acid sensitive hydrogels obtained through the incorporation of cationic groups, which ionize or protonate the ionic functional groups at acidic conditions and cause hydrogel swelling.^{3,28,29} However, the acid-labile injectable hydrogels based on the host-guest inclusion complexes for pH-triggered drug delivery are relatively less reported thus far, especially the inclusion complexes between well-defined acid-cleavable star block copolymers and α -CD.

Recently, our group synthesized several linear or star-type pH-sensitive copolymers and further prepared injectable hydrogels through the inclusion interaction of PEGylated Doxorubicin prodrug and α -CD.³⁰⁻³³ Herein, we focus on developing a new class of injectable and acid-labile hydrogels by inclusion complexes between three-armed (mPEG- α -PCL- α -)₃ and α -CD (see Scheme 1), and evaluated their potential as "smart" drug delivery carriers. These pH-sensitive supramolecular hydrogels could be formed within a few minutes in aqueous medium. Rheological studies showed that these hydrogels had a flowable character under a large stress, and the hydrogel systems exhibited unique structure-related reversible gel-sol transition properties at a certain stress. Doxorubicin hydrochloride (DOX-HCl), as a model drug, was entrapped into the hydrogels. The scission of the acetal linkages at the junction between PEG and PCL segments leads to the shedding of the hydrophilic PEG at acidic condition, resulting in the destruction of the micellization interaction. As a result, the network structure detached quickly under acid condition, and the release process exhibited a pH-dependent behavior. These pH-sensitive biocompatible drug delivery carriers are highly promising for many biomedical applications, especially in injectable hydrogels for controlled drug delivery and treatment of joint disease.



Scheme 1. Illustration of acid-cleavable hydrogel networks based on the inclusion complexes between (mPEG₄₅- α -PCL- α -)₃ and α -CD.

Experimental

Materials

Propargyl alcohol (PA, 98%, Alfa Aesar) was dried over anhydrous MgSO_4 for 24 h at room temperature and distilled under reduced pressure before use. Toluene (A.R., Sinopharm Chemical Reagent) and ϵ -caprolactone (ϵ -CL, 99%, Acros) were dried over CaH_2 for 24 h at room temperature and distilled under reduced pressure before use. Dichloromethane (CH_2Cl_2 , A.R., Sinopharm Chemical Reagent) was refluxed with CaH_2 and distilled before use. Stannous octoate [$\text{Sn}(\text{Oct})_2$, 95%, Sigma-Aldrich] was distilled under reduced pressure before use. 1, 3, 5-benzenetricarbonyl trichloride (BTT, 98%, Alfa Aesar), 4-dimethylamino pyridine (DMAP, 99%, Shanghai Medpep), poly(ethylene glycol) monomethyl ether (mPEG₄₅, $\overline{M}_n \approx 2000 \text{ g mol}^{-1}$, PDI = 1.05, TCI), 2-chloroethyl vinyl ether (CEVE, 98%, TCI), pyridinium p-toluenesulfonate (PPTS, 98%, Acros), sodium azide (NaN_3 , 98%, Sinopharm Chemical Reagent), *N,N,N',N'',N'''*-pentamethyldiethylenetriamine (PMDETA, 98%, Sigma-Aldrich), DOX-HCl (99%, Beijing Zhongshuo Pharmaceutical Technology Development) and α -CD (98%, TCI) were used without further purification. Cuprous bromide (CuBr , 95%, Sinopharm Chemical Reagent) was purified by washing in turn with acetone, glacial acetic acid, and ethanol three times, followed by drying under vacuum at room temperature for 24 h. THF (A.R., Sinopharm Chemical Reagent) was dried over KOH for at least two days and then refluxed over sodium wire with benzophenone as an indicator until the color turned purple. mPEG₄₅- α -N₃ ($\overline{M}_{n, \text{NMR}} = 2150 \text{ g mol}^{-1}$, $\overline{M}_{n, \text{GPC}} = 3600 \text{ g mol}^{-1}$, PDI = 1.06) was prepared according to the procedures reported by Hawker's group.³⁴ Milli-Q water ($18.2 \text{ M}\Omega \text{ cm}^{-1}$) was generated using a water purification system (Simplicity UV, Millipore). All the other chemicals were analytical reagents and used as received unless otherwise mentioned.

Preparation of Acid-cleavable Three-armed (mPEG- α -PCL- α)-₃

The detailed preparation procedure of three-armed star-block copolymer was reported previously by our group.³² The preparation routes can be divided into four steps: (1) synthesis of a tripropargyl-containing core molecule triprop-2-ynyl benzene-1, 3, 5-tricarboxylate (TPBTC); (2) preparation of a propargyl (PA) and acetal-functionalized PCL (PA-PCL- α -Cl); (3) synthesis of an azide and acetal-functionalized PEG (mPEG- α -N₃); (4) formation of the three-armed star-block copolymer (mPEG- α -PCL- α)-₃ via two-step CuAAC "Click" reaction.

Supramolecular Hydrogel Formation

Supramolecular hydrogels based on the inclusion complexation between various polymers and α -CD were prepared according to formulations listed in Table 1. Typically, (mPEG₄₅- α -PCL₂₇- α)-₃ (50 mg) was dissolved in Milli-Q water (550 mg) and stirred at room temperature for 24 h as a hydrogel precursor. α -CD (100 mg) was dissolved in Milli-Q water (300 mg) and added into the precursor solution with

continuous stirring. The gelation times of all the hydrogels were estimated by a vial-tilting method. The sol to gel transition was timed soon after mixing two components until no flow was observed for at least 30 s when a vial containing the hydrogel was inverted.³⁵⁻³⁷

Characterizations of the Inclusion Complexes

¹H NMR spectra were recorded on a 400 MHz NMR instrument (INOVA-400) with DMSO-*d*₆ as the solvent and tetramethylsilane (TMS) as the internal reference. Wide angle X-ray diffraction (WAXD) measurements were carried out on an X'Pert PRO Multiple Crystals (powder) X-ray Diffractometer using a Ni-filtered Cu K α radiation (λ : 1.54056 Å; voltage: 40 kV; current: 40 mA) at room temperature. The freeze-dried samples were mounted on a circular sample holder and scanned from 5 to 35° (2 θ). Differential scanning calorimetry (DSC) analysis was performed under nitrogen using a Q200 instrument (TA) at a cooling rate of 10 °C min⁻¹.

Morphologies of Lyophilized Hydrogels

In order to observe the interior morphologies of lyophilized hydrogels intuitively, the hydrogel samples were quickly frozen in liquid nitrogen and freeze-dried under vacuum at -45 °C. The freeze-dried hydrogels were then fractured carefully, and the interior morphologies of the hydrogels were visualized using a scanning electron microscope (SEM, S-4700, Hitachi). Before the SEM observation, the hydrogel samples were fixed on a copper stub and coated with gold.

Rheological Measurements

The dynamic rheological analysis was conducted using a RS 6000 rheometer (Thermo Haake) at 25 °C with parallel plate geometry (PP20H, 20 mm diameter, 0.1 mm gap). The hydrogel samples that had been aged for 24 h were carefully transferred from the glass bottle to the rheometer. Oscillatory stress sweeps were performed to determine the linear viscoelastic region profiles of the hydrogels by applying increasing shear stress logarithmically from 0.1 Pa at a fixed angular frequency (ω) of 1 rad s⁻¹ at 25 °C. Once the region where G'/G'' crossover occurred, the applied shear stress was reduced to 1.0 Pa (within the linear viscoelastic range of each sample) and tracked the structure recovery by oscillatory time sweeps of hydrogels at the same angular frequency and temperature. Also, we subjected the hydrogels to oscillatory frequency sweeps at a constant shear stress (1.0 Pa, within the linear viscoelastic range of each sample) and temperature (25 °C), the oscillatory frequency was increased from 0.1 to 100 rad s⁻¹.

Preparation of DOX-HCl-loaded Hydrogels

Typically, (mPEG₄₅- α -PCL₂₇- α)-₃ copolymer (100 mg) and DOX-HCl (20 mg) were dissolved in Milli-Q water (1100 mg) and stirred at room temperature for 24 h. α -CD (200 mg), which was dissolved in Milli-Q water (600 mg), was then added into the above-prepared solution under vigorous

stirring to induce supramolecular gelation. The mixed solution was then incubated at 25 °C for another 24 h, allowing the mixture to form the DOX·HCl-loaded hydrogel.

In Vitro DOX·HCl Release

The release profiles of DOX·HCl from drug-loaded hydrogels were investigated at 37 °C in an acetate buffer solution (pH 5.0, 10 mM) and a phosphate buffer solution (pH 7.4, 10 mM). Typically, prepared drug-loaded hydrogel (300 mg) was added into a tubelet (0.6 mL) and transferred into a dialysis membrane tube (MWCO 12000-14000), which was immersed into a tube containing 20 mL of corresponding buffer solution. The tube was put in a shaking water bath at 37 °C. At predetermined intervals, 5 mL of release medium was taken out and replenished with an equal volume of fresh corresponding buffer solution. Fluorescence measurement was carried out to determine the released DOX·HCl concentration. The solution was measured by fluorescence spectroscopy (FLS920, Edinburgh) with excitation at 480 nm and emission at 560 nm, and the slit width was set at 5 nm. All the release experiments were conducted in triplicate in the dark and the results were the average values with standard deviation.

Results and Discussion

Supramolecular Hydrogel Formation

Recently, the application as injectable hydrogels for supramolecular hydrogels based on host-guest chemistry has received much attention. As reported, the supramolecular hydrogels can be formed within a few minutes in aqueous solution

after mixing the PEG-contained copolymers with α -CD.^{23,24} The molecular feed ratio of EG unit to α -CD is a vital design parameter that affects the cross-linking density and hydrogel formation.³⁸ As reported, the inclusion complexes can be formed between PEG and α -CD with a stoichiometry of 2:1 (EG unit: α -CD) by host-guest interaction.^{37,39,40}

In the present study, supramolecular hydrogels were obtained by adjusting the feed ratios of EG unit to α -CD (from 2.4:1 to 5.6:1) for various block polymers, leaving uncovered hydrophilic chains function as water soluble segments. As shown in Scheme 1, once predetermined α -CD solution was added into the precursor polymer solution, the mixture became cloudy rapidly. Viscosity of the mixture solution gradually increased with simultaneous increase in turbidity with time going on. Finally, the turbid mixture became stagnant and formed a three-dimensional cross-linked network hydrogel. The inclusion complexes formed between the PEG block and α -CD are thought to aggregate into necklace-like crystalline polypseudorotaxanes and act as physical cross-linking joints for the hydrogels, while remaining uncovered hydrophilic chains function as water absorbing segments. Also, the micellization of the amphiphilic polymers in aqueous solution plays an important role in inducing the gelation of hydrogels. The gelation times for all the hydrogels were estimated by a vial-tilting method and are shown in Table 1. Compared the gelation time for GEL-(EC₂₇)₃-1, GEL-(EC₂₇)₃-2, and GEL-(EC₂₇)₃-3, the results showed that the gelation process required a longer time for the polymers at lower concentrations. However, when α -CD solution was mixed with mPEG₄₅ solution, only white precipitate was observed, which could be attributed to the low molecular weight of PEG and high feed ratio of EG unit to α -CD (9.7:1).^{37,39}

Table 1 Hydrogel formulations and corresponding gelation time

Hydrogel ^{a)}	Polymers	$W_{\text{polymer}}/\text{mg}$	$W_{\alpha\text{-CD}}/\text{mg}$	Feed ratio (wt %)		Gelation time/s ^{b)}
				Polymer: α -CD	Molecular ratio EG unit: α -CD	
GEL-E	mPEG ₄₅	50	100	5:10	9.7:1	—
GEL-EC ₂₇	mPEG ₄₅ - α -PCL ₂₇ - α -Cl	50	100	5:10	4.1:1	165
GEL-(EC ₁₈) ₃	(mPEG ₄₅ - α -PCL ₁₈ - α) ₃	50	100	5:10	5.0:1	88
GEL-(EC ₂₇) ₃ -1	(mPEG ₄₅ - α -PCL ₂₇ - α) ₃	30	100	3:10	2.4:1	115
GEL-(EC ₂₇) ₃ -2	(mPEG ₄₅ - α -PCL ₂₇ - α) ₃	50	100	5:10	4.0:1	95
GEL-(EC ₂₇) ₃ -3	(mPEG ₄₅ - α -PCL ₂₇ - α) ₃	70	100	7:10	5.6:1	92

^{a)} Hydrogel formulations are noted as GEL-(polymer abbreviation)-x, where E represents mPEG₄₅, EC₂₇ represents mPEG₄₅- α -PCL₂₇- α -Cl, (EC₁₈)₃ represents (mPEG₄₅- α -PCL₁₈- α)₃, (EC₂₇)₃ represents (mPEG₄₅- α -PCL₂₇- α)₃, 18 and 27 represent the degree of polymerization of PCL, and x distinguishes the different formulations within a polymer series. ^{b)} Estimated from vial-tilting technique.

Characterization of the Inclusion Complexes

The formation of the inclusion complexes between PEG-contained polymers and α -CD was characterized by ¹H NMR, WAXD, and DSC measurements. Fig. 1 displays the ¹H NMR spectra of α -CD and lyophilized GEL-(EC₂₇)₃-2, respectively. As shown in Fig. 1(A), characteristic resonance signals at δ 3.27 ppm, δ 3.39 ppm, δ 3.57-3.68 ppm, δ 3.77 ppm, δ 4.50 ppm, δ 4.79 ppm, δ 5.44 ppm, and δ

5.52 ppm can be ascribed to the protons of commercially available α -CD, respectively. Also, the resonance signals attributed to the protons of α -CD, TPBTC, PEG and PCL segments can be observed clearly in Fig. 1(B), and relative resonance signals were also labeled.

WAXD measurement was widely used in substantiating the formation of the crystalline inclusion complexes between PEG-contained polymers (guest molecule) and α -CD (host

molecule).^{23,38} Fig. 2 shows the WAXD patterns of α -CD (Fig. 2(A)), (mPEG₄₅-*a*-PCL₂₇-*a*)₃ (Fig. 2(B)) and freeze-dried inclusion complexes (Fig. 2(C-H)). The results showed that α -CD exhibited multiple diffraction peaks corresponding to the crystalline form (Fig. 2(A)), and (mPEG₄₅-*a*-PCL₂₇-*a*)₃ displayed diffraction maxima at $2\theta = 19.1^\circ, 21.3^\circ, 23.3^\circ$ and 23.7° (Fig. 2(B)), indicating the coincident crystallization of PEG (19.1°, 23.3°) and PCL (21.3°, 23.7°) blocks. For the investigated inclusion complexes, all patterns (Fig. 2(C-H)) exhibited a number of sharp reflections and the main peaks are at 19.8° and 22.6° . Moreover, there was no obvious peak from α -CD crystals in the pattern of the complexes. These results demonstrated that a large number of α -CD molecules were threaded onto the PEG chains, and formed the channel-type structure of a crystalline necklace-like complex. The WAXD pattern of GEL-E (Fig. 2(C)) showed characteristic diffraction maxima of crystalline PEG at $2\theta = 19.1^\circ, 23.3^\circ$, which can be attributed to high feed ratio of EG unit to α -CD (9.7:1), resulting in an ocean of uncovered hydrophilic EG units. As shown in Fig. 2(D-H), the characteristic diffraction maxima related to PEG were rarely detected, whereas those signals corresponding to crystalline PCL can be detected in Fig. 2(D, F, G, H). Remarkably, the characteristic diffraction maxima intensity of crystalline PCL increased by increasing the polymer proportion, whereas those related to GEL-(EC₁₈)₃ rarely detected. This is in agreement with the result reported before.³²

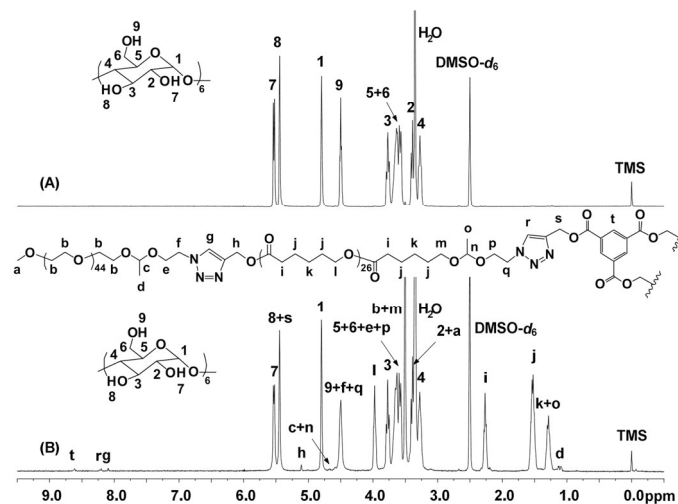


Fig. 1 ¹H NMR spectra of (A) α -CD and (B) lyophilized GEL-(EC₂₇)₃-2 in DMSO-*d*₆.

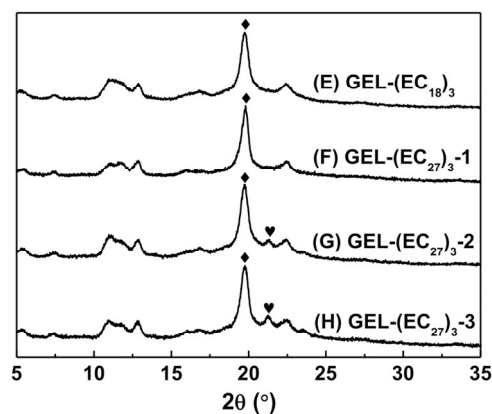
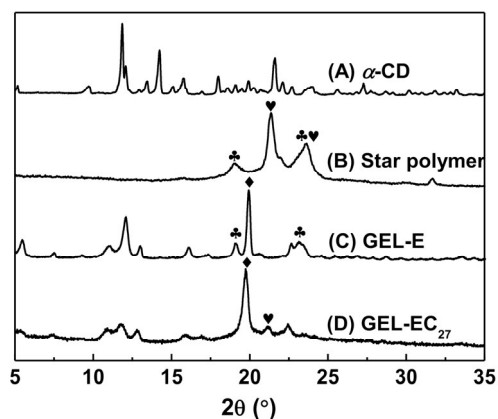


Fig. 2 WAXD patterns of (A) α -CD, (B) (mPEG₄₅-*a*-PCL₂₇-*a*)₃,³² (C) lyophilized GEL-E, (D) lyophilized GEL-EC₂₇, (E) lyophilized GEL-(EC₁₈)₃, (F) lyophilized GEL-(EC₂₇)₃-1, (G) lyophilized GEL-(EC₂₇)₃-2, and (H) lyophilized GEL-(EC₂₇)₃-3. The characteristic X-ray diffraction peaks of PEG block, PCL block and the inclusion complexes are labeled with \clubsuit , \heartsuit , and \diamond , respectively.

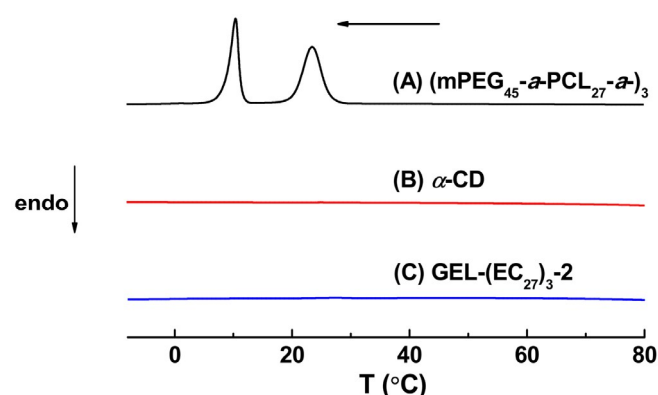


Fig. 3 DSC thermograms of (A) (mPEG₄₅-*a*-PCL₂₇-*a*)₃, (B) α -CD, and (C) lyophilized GEL-(EC₂₇)₃-2 with a $10^\circ\text{C min}^{-1}$ scanning rate in the second cooling run.

The thermal properties of (mPEG₄₅-*a*-PCL₂₇-*a*)₃, α -CD, and lyophilized GEL-(EC₂₇)₃-2 were characterized by DSC technique. Fig. 3 displays the DSC thermograms of (mPEG₄₅-*a*-PCL₂₇-*a*)₃ (Fig. 3(A)), α -CD (Fig. 3(B)), and lyophilized GEL-(EC₂₇)₃-2 (Fig. 3(C)), respectively. As shown in Fig. 3(A), the coexistence of two crystalline phases was suggested by the presence of well separated crystallization peaks, which can be explained by the fractionated crystallization.³² However, the DSC trace of α -CD showed no crystallization peak in the temperature range (Fig. 3(B)). It should be notable that there was no crystallization peaks corresponding to PEG and PCL crystals observed in the DSC thermogram of lyophilized GEL-(EC₂₇)₃-2 (Fig. 3(C)). The crystallization behavior can be explained by the host-guest interaction. As PEG chains are included, they are isolated in the α -CD inner core and form a new necklace-like crystalline polypseudorotaxanes with the disappearance of any melting behavior, which agrees well with the results reported by other researchers.^{37,38,41-43} The WAXD pattern of the lyophilized GEL-(EC₂₇)₃-2 showed characteristic diffraction maxima of PCL, while the corresponding peak can't be found in the DSC curve. This is because both of the PEG and PCL segments are partly crystalline and various amorphous state chains existed in the GEL-(EC₂₇)₃-2. In addition, the new necklace-like crystals may have strong restrictions to PEG and PCL chains and hinder their crystallization.

Morphologies of Lyophilized Hydrogels

The morphologies of various lyophilized hydrogels were observed by SEM measurement. As shown in Fig. 4(B-F), the SEM images of lyophilized supramolecular hydrogels exhibited porous spongelike structure. The average pore size of the hydrogels varied with the content of hydrophilic and hydrophobic segments. When the DP of hydrophobic PCL segments increased from 18 (Fig. 4(C)) to 27 (Fig. 4(E)), the average pore size decreased. These pore size differences can be attributed to the micellization of hydrogels, and the hydrophobic interactions are stronger for the polymers with longer hydrophobic segments.⁴⁴ As shown in Fig. 4(D-F), the average pore size decreased with increasing (mPEG₄₅-*α*-PCL₂₇-*α*)₃ concentration, which can be ascribed to the increasing of cross-linking density.⁴⁵ In contrast, the morphological structure of lyophilized GEL-E exhibited irregular morphology instead of porous structure (Fig. 4(A)), indicating the GEL-E was less gel-like than the other hydrogels, in accordance with the gelation time and WAXD results.

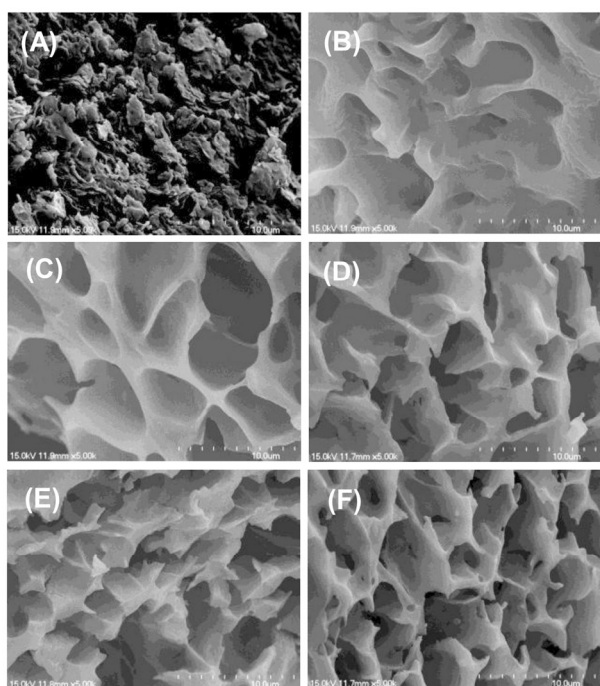


Fig. 4 SEM images of (A) lyophilized GEL-E, (B) lyophilized GEL-EC₂₇, (C) lyophilized GEL-(EC₁₈)₃, (D) lyophilized GEL-(EC₂₇)₃-1, (E) lyophilized GEL-(EC₂₇)₃-2, and (F) lyophilized GEL-(EC₂₇)₃-3.

Rheological Properties of Supramolecular Hydrogels

The rheological measurement was employed to investigate the rheological properties of supramolecular hydrogels. The rheological characterization data are presented in Table 2. Oscillatory stress sweep measurements were performed to determine the linear viscoelastic region profiles of the

hydrogels by applying increasing shear stress logarithmically (Fig. 5). Inset is an expansion of the region where G'/G'' crossover occurred and the applied shear stress at this point is defined as yield point (σ_y), which is an important parameter to characterize the hydrogel network structure. Also, small yield point values can be attributed to easier crosslink dissociation.⁴⁶ As shown in Fig. 5, the results showed that GEL-(EC₂₇)₃-2 had a larger yield point than GEL-(EC₂₇)₃-1 and GEL-(EC₂₇)₃-3, indicating a larger linear viscoelastic region. The phenomena implied that more energy is required to disrupt the columnar crystalline cross-linking points within GEL-(EC₂₇)₃-2 than in GEL-(EC₂₇)₃-1 and GEL-(EC₂₇)₃-3. Notably, more energy is required to disrupt the columnar crystalline cross-linking points within GEL-(EC₂₇)₃-2 than in GEL-EC₂₇, which is owing to a fair thermodynamic stability of star polymeric micelles in aqueous medium.

A good recovery property of the hydrogel network after structure destruction as a result of high shear stresses during injection is an important factor to ensure successful application in injectable hydrogels matrix. In particular, the hydrogel network should recover as fast as possible and be able to withstand mechanical stress caused by surrounding tissues and body fluids after injection.¹³ The rheometer was used to simulate the injection process by subjecting the hydrogels to high shear stress until their hydrogel network collapsed, and then monitoring their structure recovery by applying a small shear stress (within the linear viscoelastic range). In this study, the initial G' after gelation were found to be about 323, 205, 462, 44, 1176, and 29 Pa (Fig. 5 and Fig. 6) for GEL-E, GEL-EC₂₇, GEL-(EC₁₈)₃, GEL-(EC₂₇)₃-1, GEL-(EC₂₇)₃-2, and GEL-(EC₂₇)₃-3 at a small shear stress (1.0 Pa), respectively. Besides, for all the systems, their G' values were above the G'' ones. When a large stress (above the yield point) was applied, G' decreased dramatically close to zero, and smaller than G'' as well, indicating the disruption of the hydrogel network. The applied shear stress was then reduced to 1.0 Pa to monitor the structure recovery by oscillatory time sweep measurements. The G' and G'' values simultaneously increased with time going on, and G' increased faster than G'' as a result of gradual structure recovery. Finally, G' increased larger than G'' , suggesting the recovery of the hydrogel network. As shown in Fig. 6, the values finally recovered to their original moduli within 200 s, showing a very fast recovery process of the hydrogel system, indicating potential application in injectable hydrogels for drug delivery carriers.

Viscosity (η) is another important parameter that indirectly characterizes the hydrogel network structure. It can be calculated according to formula (1), where η is the viscosity, σ is the shear stress, and $\dot{\gamma}$ represents the shear rate.

$$\eta = \frac{\sigma}{\dot{\gamma}} \quad (1)$$

Table 2 Rheological data of hydrogels obtained from the rheological measurements.

Hydrogel	σ_y/Pa ^{a)}	G'/Pa ^{b)}	G''/Pa ^{b)}	G'/Pa ^{c)}	G''/Pa ^{c)}	$\eta_1/\text{Pa}\cdot\text{s}$ ^{d)}	$\eta_2/\text{Pa}\cdot\text{s}$ ^{e)}
GEL-E	19.2 ± 1.1	323.3 ± 6.6	123.8 ± 1.5	183.0 ± 18.2	63.2 ± 4.2	337.0 ± 91.6	193.7 ± 18.5
GEL-EC ₂₇	64.2 ± 3.3	204.9 ± 3.0	21.2 ± 1.0	107.9 ± 4.2	13.5 ± 0.8	277.6 ± 4.3	108.7 ± 4.2
GEL-(EC ₁₈) ₃	175.4 ± 9.8	462.2 ± 3.8	56.2 ± 5.0	498.8 ± 24.1	53.6 ± 4.1	1036 ± 26.9	501.6 ± 24.4
GEL-(EC ₂₇) ₃ -1	6.9 ± 0.4	44.4 ± 0.2	4.8 ± 0.2	32.0 ± 0.1	4.1 ± 0.1	40.2 ± 0.9	32.2 ± 0.1
GEL-(EC ₂₇) ₃ -2	149.7 ± 8.3	1176.0 ± 45.0	354.6 ± 17.7	954.6 ± 129.3	242.1 ± 74.2	993.0 ± 165.5	795.0 ± 125.0
GEL-(EC ₂₇) ₃ -3	58.0 ± 3.2	29.1 ± 2.3	5.3 ± 0.2	71.2 ± 7.6	9.2 ± 0.5	280.4 ± 8.3	61.5 ± 7.0

^{a)} Yield point, defined as the applied shear stress value at G'/G'' crossover. ^{b)} Elastic modulus (G') and viscous modulus (G'') determined by oscillatory stress sweep measurements at the shear stress of 1.0 Pa. ^{c)} G' and G'' determined by oscillatory time sweep measurements at constant $\sigma = 1.0$ Pa soon after the appearance of the yield point for 200 s. ^{d)} Viscosity (η_1) determined by oscillatory stress sweep measurements at the shear rate of 0.1 s^{-1} . ^{e)} η_2 determined by oscillatory time sweep measurements at constant $\sigma = 1.0$ Pa soon after the appearance of the yield point for 200 s.

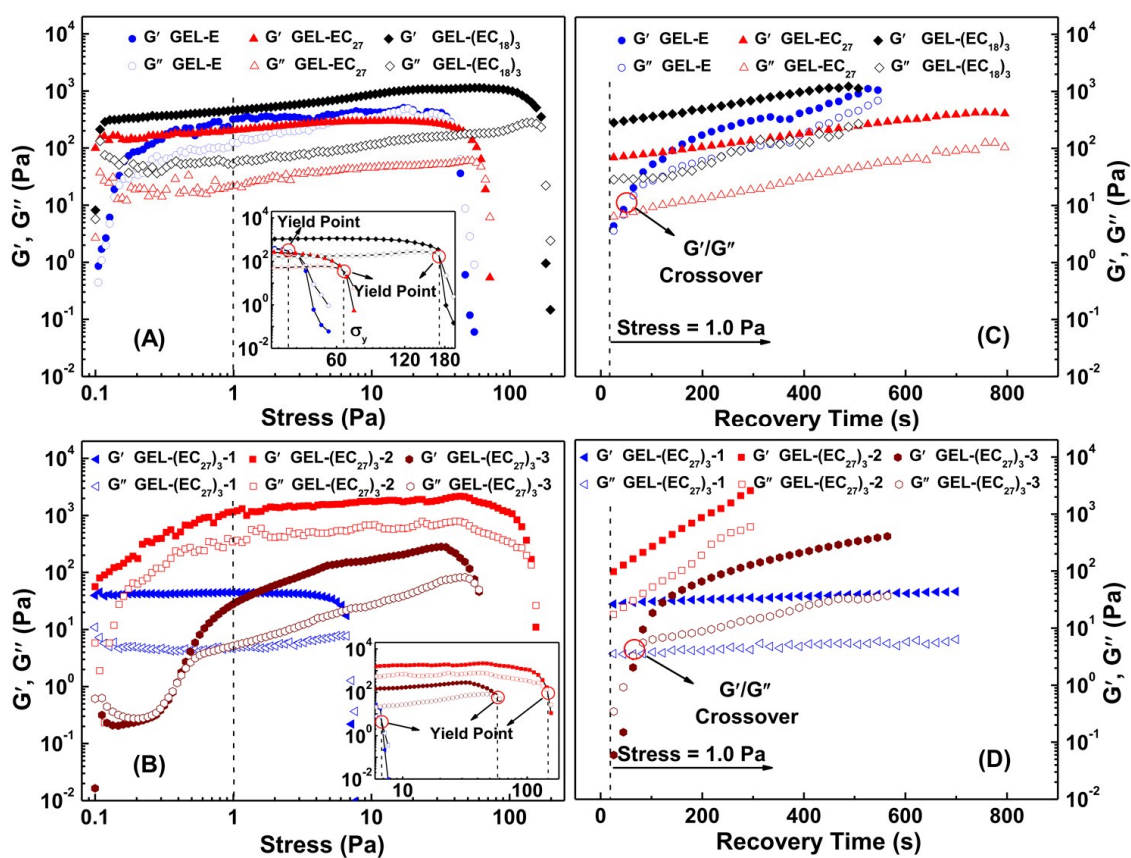


Fig. 5 Oscillatory stress sweep measurements of various hydrogels at 25 °C and constant $\omega = 1 \text{ rad s}^{-1}$ (A and B). Two Insets are expansions of the region where G'/G'' crossover occurred and the applied shear stress at this point is defined as yield point (σ_y). Oscillatory time sweep measurements of various hydrogels at 25 °C, $\omega = 1 \text{ rad s}^{-1}$ and $\sigma = 1.0$ Pa soon after the appearance of the yield point (C and D).

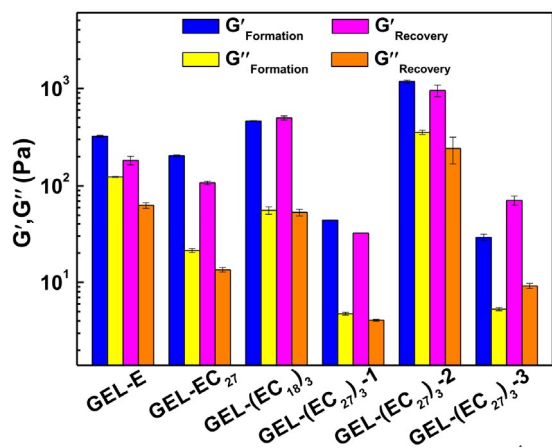


Fig. 6 $G'_{\text{Formation}}$ and $G''_{\text{Formation}}$ determined by oscillatory stress sweep measurements at the shear stress of 1.0 Pa. G'_{Recovery} and G''_{Recovery} determined by oscillatory time sweep measurements at constant $\sigma = 1.0$ Pa soon after 200 s of the appearance of the yield point.

Fig. 7 shows the relationship between apparent viscosity and shear rate for the supramolecular hydrogels. Remarkably, the viscosity for the supramolecular hydrogels decreased with the increasing of shear rate, suggesting a shear-thinning behavior. This confirms that applied required energy can disrupt the network structure, resulting in the decreasing of the viscosity. Also, the structure recovery can be monitored by a viscosity technique. As shown in Fig. 7 and Fig. 8, the viscosity finally recovered to their original values within 200 s. This result can be explained by the nature of supramolecular hydrogel systems, since the cross-links of such systems are transformable and recoverable.

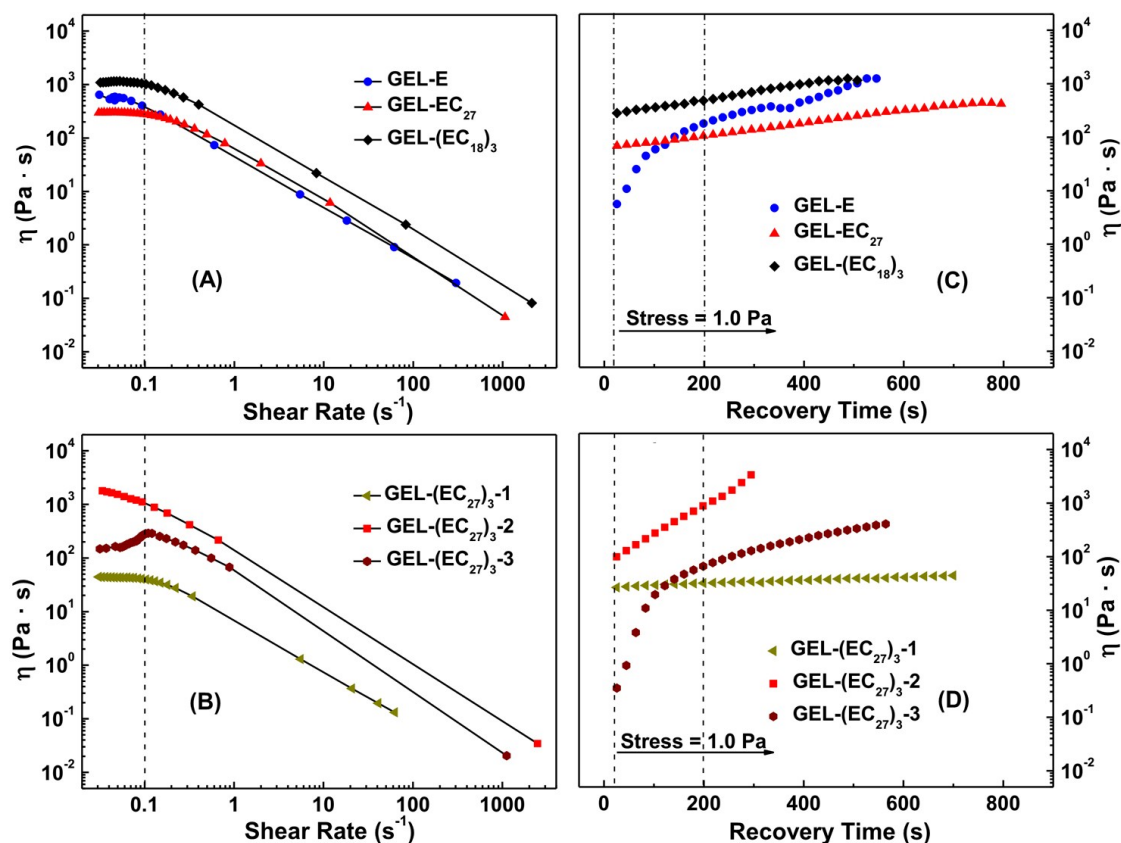


Fig. 7 Relationship between apparent viscosity and shear rate for the supramolecular hydrogels (A and B) and creep recovery measurements (C and D).

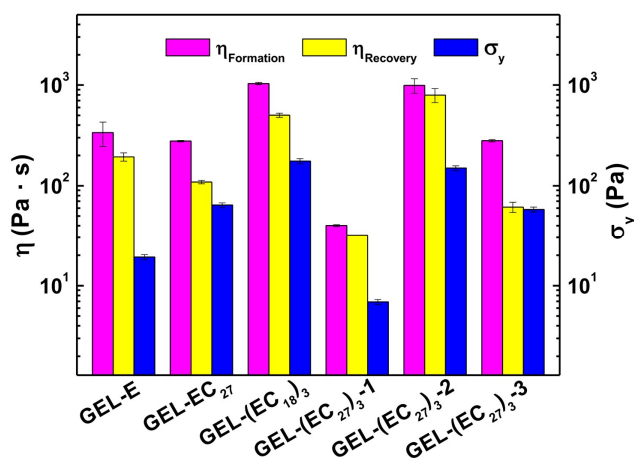


Fig. 8 Viscosity (η) determined by oscillatory stress sweep measurements at the shear rate of 0.1 s^{-1} and at constant $\sigma = 1.0 \text{ Pa}$ soon after the appearance of the yield point for 200 s. Yield point determined by oscillatory stress sweep measurements.

Oscillatory frequency sweep measurements were measured to further characterize the rheological behaviors of the hydrogels. As shown in Fig. 9, the G' values of GEL-EC₂₇, GEL-(EC₁₈)₃, GEL-(EC₂₇)₃-2, and GEL-(EC₂₇)₃-3 were hardly changed and were always larger than G'' during the frequency was increased from 0.1 to 100 rad s^{-1} , indicating a fairly stable hydrogel network system. Notably, GEL-E and GEL-(EC₂₇)₃-1 exhibited greater frequency dependency in their G' and G'' values. G' of GEL-E was very close to G'' at low frequency, however, G' increased faster than G'' with increasing frequency, from which we speculate that the GEL-E is less gel-like than the other hydrogels. That was in accordance with the results of gelation time, WAXD, and SEM. In contrast, GEL-(EC₂₇)₃-1 had very little change in their G' values and were always larger than G'' at low frequency, and exhibited a G'/G'' crossover at around 85 rad s^{-1} . As mentioned above, the complexed PEG units worked as physical cross-linking points, while the uncomplexed units maintain their hydrophilicity. The frequency dependent behavior for GEL-(EC₂₇)₃-1 can be attributed to the low feed ratio of EG unit to α -CD (2.4:1), as most of the EG units formed complexed hydrophobic parts to maintain rarely no uncomplexed hydrophilic segments in the hydrogel system. As a result, less energy is required to disrupt the network structure.

The rheological behaviors of the supramolecular hydrogels based on the inclusion complexes between the star block copolymers and α -CD demonstrated that they have great potential application in injectable hydrogels as drug carriers due to their good structure recovery properties. Oscillatory stress sweep measurements showed that these hydrogels exhibited a flowable character under a large stress. The hydrogel systems exhibited unique structure-related reversible gel-sol transition properties at a certain stress, and started to restore their network structure immediately after removing the applied high shear stress. Furthermore, oscillatory frequency sweep measurements showed that hydrogels based on star block copolymers are essentially elastic in response to small stresses over a frequency range that covers everyday activities such as walking and running.^{13,47}

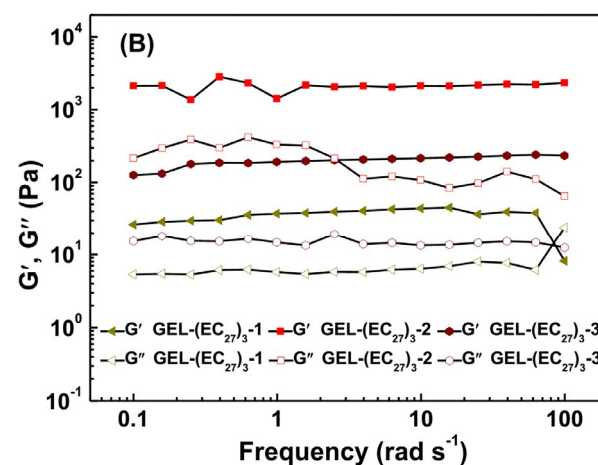
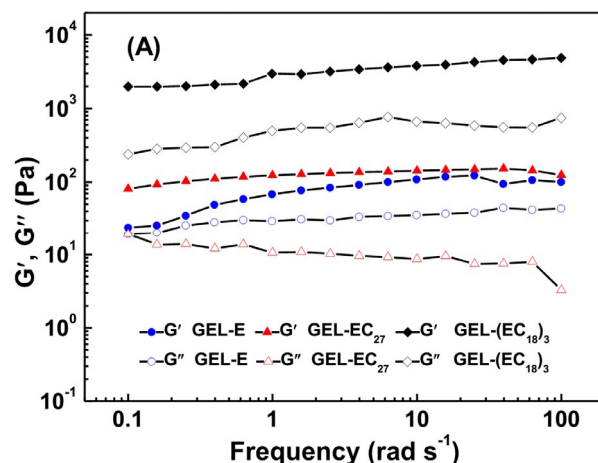


Fig. 9 Oscillatory frequency sweep measurements of various hydrogels at $25 \text{ }^\circ\text{C}$ and constant $\sigma = 1.0 \text{ Pa}$.

In Vitro DOX·HCl Release

The potential application of supramolecular hydrogel as a new injectable drug delivery system for the encapsulation and sustained release of DOX·HCl was investigated. DOX·HCl was encapsulated in the hydrogel matrix during the gelation process. The *in vitro* cumulative release of DOX·HCl from hydrogels were performed at $37 \text{ }^\circ\text{C}$ in two different buffer solutions (pH 5.0 and 7.4) to study the effect of pH values on drug release, and the cumulative release percentage of DOX·HCl was calculated based on Beer-Lambert's law:³⁷

$$\text{Released (\%)} = \frac{M_{\text{released}}}{M_{\text{initial}}} \times 100 \quad (2)$$

where M_{released} is the cumulative release weight of DOX·HCl, M_{initial} is the initial weight of DOX·HCl encapsulated in the hydrogel.

We have investigated the acid-cleavable behavior of the star-block copolymer (mPEG- α -PCL- α)₃ by ^1H NMR, GPC and DLS measurements at different pH values in the present work. The star-block copolymer can be degraded into the corresponding homopolymers within 24 h by the scission of acetal linkages under acidic conditions.³² Fig. 10 shows the *in vitro* cumulative DOX·HCl release curves for GEL-(EC₂₇)₃-2 at different pH values. Remarkably, the results showed that DOX·HCl was released from hydrogels much faster at acidic condition than at physiological condition.

Furthermore, the drug release profile of GEL-(EC₂₇)₃-2 exhibited a triphasic pattern at pH 5.0. The release process had a fast drug release rate ($S_1 = 1.06 \text{ h}^{-1}$) within initial 30 h (about 45% of drug was released), a moderate drug release rate ($S_2 = 0.35 \text{ h}^{-1}$) within the next 100 h (about 35% of drug was released), and then a slow drug release rate ($S_3 = 0.06 \text{ h}^{-1}$) within the next 140 h (approximately 10% of drug was released). In contrast, a slow and steady drug release rate ($S = 0.04 \text{ h}^{-1}$) and minimal DOX-HCl release was observed at pH 7.4 after 270 h under the same condition. The pH-sensitive release behavior of hydrogels could be ascribed to the scission of the acetal linkages at the junction between PEG and PCL segments leads to the shedding of the hydrophilic PEG at acidic condition.

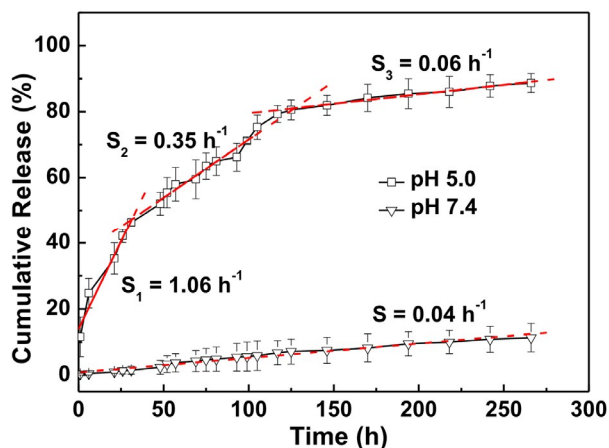


Fig. 10 *In vitro* cumulative release of encapsulated DOX-HCl from GEL-(EC₂₇)₃-2 at 37 °C at different conditions: pH 5.0 buffer solution and pH 7.4 buffer solution.

To elucidate the release mechanism of encapsulated DOX-HCl, the cumulative drug-release amounts were fitted using calculation (3)^{37,48,49}

$$M_t / M_\infty = kt^n \quad (\text{for } M_t / M_\infty \leq 0.6) \quad (3)$$

where M_t and M_∞ are the cumulative drug-release amount at t and equilibrium, respectively, k is the rate constant relating to the properties of the hydrogel matrix and the drug, and n is the release exponent characterizing the transport mechanism. There are mainly four distinguishable modes of diffusion: pseudo-Fickian transport behavior ($n < 0.5$), Fickian or Case I behavior ($n = 0.5$), Case III behavior ($0.5 < n < 1$), and non-Fickian or Case II mode of transport ($n = 1$).⁴⁹ Taking the logarithm of equation (3), calculation (4) was obtained.

$$\log(M_t / M_\infty) = n \log(t) + \log(k) \quad (4)$$

As listed in Table 3, the n , k , and corresponding determination coefficients (R^2) values were obtained by plotting $\log(M_t/M_\infty)$ versus $\log(t)$. The release exponents of GEL-(EC₂₇)₃-2 were calculated to be 0.92 ± 0.03 and 0.39 ± 0.01 at pH 7.4 and 5.0, respectively. The results indicated that encapsulated DOX-HCl released from GEL-(EC₂₇)₃-2 at pH 7.4 by an anomalous transport process (Case III behavior), and the structure relaxation is comparable to diffusion.⁴⁹⁻⁵¹ In contrast, the transport mechanism of GEL-(EC₂₇)₃-2 at pH 5.0 was a pseudo-Fickian behavior of diffusion where sorption curves resemble Fickian curves, but the approach to final equilibrium is very slow. This phenomenon can

be ascribed to the scission of the acetal linkages at the junction between PEG and PCL segments leads to the shedding of the hydrophilic PEG at acidic condition, resulting in the destruction of the micellization interaction. As a result, the network structure of GEL-(EC₂₇)₃-2 detached quickly under acid condition, and the release process exhibited a fast drug-release rate.

Table 3 Release characteristics of encapsulated DOX-HCl from GEL-(EC₂₇)₃-2.

pH	k	n	R^2	Transport mechanism
7.4	0.0067 ± 0.0009	0.92 ± 0.03	0.98	Case III
5.0	0.13 ± 0.01	0.39 ± 0.01	0.98	pseudo-Fickian

Conclusions

A novel acid-cleavable and injectable supramolecular hydrogels based on the inclusion complexes between the acid-cleavable (mPEG- α -PCL- α)₃ and α -CD were prepared within a few minutes. The inclusion complexes aggregated into necklace-like crystalline polypseudorotaxanes and acted as physical cross-linking joints for the hydrogels, while remaining uncovered hydrophilic chains functioned as water absorbing segments. These hydrogels showed a flowable character under a large stress and unique structure-related reversible gel-sol transition properties at a certain stress, while they started to restore their network structure immediately after removing of the applied high shear stress. In addition, these hydrogels essentially elastic in response to small stresses over a frequency range that covers everyday activities such as walking and running. Importantly, the lyophilized hydrogels exhibited porous spongelike structure and could be used as drug delivery depots. The *in vitro* drug release showed that DOX-HCl was released from drug-loaded hydrogels in a controlled and pH-dependent manner. These pH-sensitive hydrogels are highly promising for many biomedical applications, especially in controlled drug delivery injectable hydrogels and treatment of joint disease.

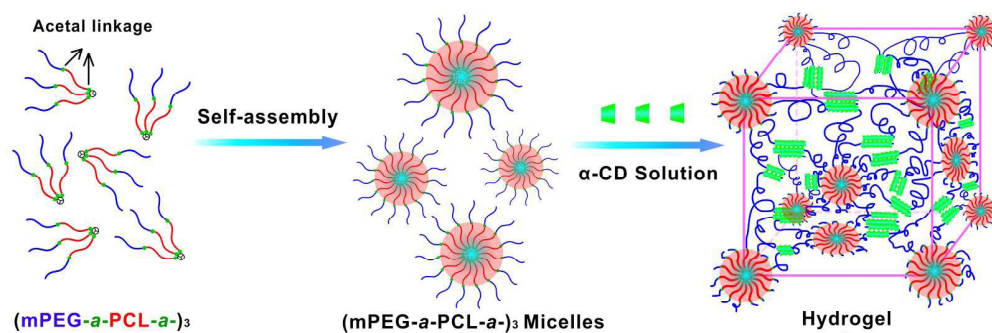
Acknowledgements

We gratefully acknowledge financial supports from the National Natural Science Foundation of China (21374066 and 21304061), the Major Program of the Natural Science Project of Jiangsu Higher Education Institutions (15KJA150007), the Natural Science Foundation of Jiangsu Province (BK20130286), the Natural Science Foundation of Jiangsu Higher Education Institutions (13KJB150034), a Project Funded by the Priority Academic Program Development (PAPD) of Jiangsu Higher Education Institutions, Suzhou Science and Technology Program for Industrial Application Foundation (SYG201429), and Soochow-Waterloo University Joint Project for Nanotechnology from Suzhou Industrial Park.

References and Notes

1. Y. Qiu and K. Park, *Adv. Drug Delivery Rev.*, 2001, **53**, 321-339.
2. A. S. Hoffman, *Adv. Drug Delivery Rev.*, 2002, **54**, 3-12.
3. T. R. Hoare and D. S. Kohane, *Polymer*, 2008, **49**, 1993-2007.
4. A. S. Hoffman, *Adv. Drug Delivery Rev.*, 2012, **64**, 18-23.
5. Y. Qiu and K. Park, *Adv. Drug Delivery Rev.*, 2012, **64**, 49-60.
6. L. Yu and J. D. Ding, *Chem. Soc. Rev.*, 2008, **37**, 1473-1481.
7. C. L. He, S. W. Kim and D. S. Lee, *J. Controlled Release*, 2008, **127**, 189-207.
8. A. S. Sawhney, C. P. Pathak and J. A. Hubbell, *Macromolecules*, 1993, **26**, 581-587.
9. S. J. de Jong, S. C. De Smedt, M. W. C. Wahls, J. Demeester, J. J. Kettenes-van den Bosch and W. E. Hennink, *Macromolecules*, 2000, **33**, 3680-3686.
10. Z. S. Ge, J. M. Hu, F. H. Huang and S. Y. Liu, *Angew. Chem.*, 2009, **121**, 1830-1834.
11. L. Sun, W. Liu and C. M. Dong, *Chem. Commun.*, 2011, **47**, 11282-11284.
12. Z. B. Li, H. Yin, Z. X. Zhang, K. L. Liu and J. Li, *Biomacromolecules*, 2012, **13**, 3162-3172.
13. K. L. Liu, J. L. Zhu and J. Li, *Soft Matter*, 2010, **6**, 2300-2311.
14. E. Ruel-Gariépy and J. C. Leroux, *Eur. J. Pharm. Biopharm.*, 2004, **58**, 409-426.
15. S. Toledano, R. J. Williams, V. Jayawarna and R. V. Ulijn, *J. Am. Chem. Soc.*, 2006, **128**, 1070-1071.
16. A. K. Bajpai, S. K. Shukla, S. Bhanu and S. Kankane, *Prog. Polym. Sci.*, 2008, **33**, 1088-1118.
17. F. Lee, J. E. Chung and M. Kurisawa, *Soft Matter*, 2008, **4**, 880-887.
18. J. E. Frith, A. R. Cameron, D. J. Menzies, Peter Ghosh, D. L. Whitehead, S. Gronthos, A. C. W. Zannettino and J. J. Cooper-White, *Biomaterials*, 2013, **34**, 9430-9440.
19. Y. H. Ma, J. J. Yang, B. L. Li, Y. W. Jiang, X. L. Lu and Z. Chen, *Polym. Chem.*, 2016, DOI: 10.1039/c5py01773d.
20. K. L. Liu, Z. X. Zhang and J. Li, *Soft Matter*, 2011, **7**, 11290-11297.
21. H. H. Kuang, H. Y. He, Z. Y. Zhang, Y. X. Qi, Z. G. Xie, X. B. Jing and Y. B. Huang, *J. Mater. Chem. B*, 2014, **2**, 659-667.
22. F. Li, J. L. He, M. Z. Zhang and P. H. Ni, *Polym. Chem.*, 2015, **6**, 5009-5014.
23. K. M. Huh, T. Ooya, W. K. Lee, S. Sasaki, I. C. Kwon, S. Y. Jeong and N. Yui, *Macromolecules*, 2001, **34**, 8657-8662.
24. J. Li, X. Li, Z. H. Zhou, X. P. Ni and K. W. Leong, *Macromolecules*, 2001, **34**, 7236-7237.
25. S. Ganta, H. Devalapally, A. Shahiwala and M. Amiji, *J. Controlled Release*, 2008, **126**, 187-204.
26. E. S. Lee, Z. G. Gao and Y. H. Bae, *J. Controlled Release*, 2008, **132**, 164-170.
27. C. Deng, Y. J. Jiang, R. Cheng, F. H. Meng and Z. Y. Zhong, *Nano Today*, 2012, **7**, 467-480.
28. P. Gupta, K. Vermani and S. Garg, *Drug Discov. Today*, 2002, **7**, 569-579.
29. D. Schmaljohann, *Adv. Drug Delivery Rev.*, 2006, **58**, 1655-1670.
30. H. R. Wang, J. L. He, M. Z. Zhang, Y. F. Tao, F. Li, K. C. Tam and P. H. Ni, *J. Mater. Chem. B*, 2013, **1**, 6596-6607.
31. Y. Zhang, J. L. He, D. L. Cao, M. Z. Zhang and P. H. Ni, *Polym. Chem.*, 2014, **5**, 5124-5138.
32. J. Hu, J. L. He, M. Z. Zhang and P. H. Ni, *Polym. Chem.*, 2015, **6**, 1553-1566.
33. F. Li, J. L. He, M. Z. Zhang, K. C. Tam and P. H. Ni, *RSC Adv.*, 2015, **5**, 54658-54666.
34. K. Satoh, J. E. Poelma, L. M. Campos, B. Stahl and C. J. Hawker, *Polym. Chem.*, 2012, **3**, 1890-1898.
35. S. Y. Park, D. K. Han and S. C. Kim, *Macromolecules*, 2001, **34**, 8821-8824.
36. S. Y. Park, B. R. Han, K. M. Na, D. K. Han and S. C. Kim, *Macromolecules*, 2003, **36**, 4115-4124.
37. Z. C. Tian, C. Chen and H. R. Allcock, *Macromolecules*, 2013, **46**, 2715-2724.
38. C. C. Rusa and A. E. Tonelli, *Macromolecules*, 2000, **33**, 1813-1818.
39. A. Harada, J. Li and M. Kamachi, *Macromolecules*, 1993, **26**, 5698-5703.
40. A. Harada, J. Li and M. Kamachi, *Macromolecules*, 1994, **27**, 4538-4543.
41. J. Lu, I. D. Shin, S. Nojima and A. Tonelli, *Polymer*, 2000, **41**, 5871-5883.
42. Y. Xiao, J. L. He, Y. F. Tao, M. Z. Zhang, J. Hu and P. H. Ni, *Acta Polym. Sin.*, 2014, **1**, 122-130.
43. L. Y. Wu, L. Yu, X. H. Fu and Z. B. Li, *Chinese J. Polym. Sci.*, 2015, **33**, 1140-1149.
44. D. Q. Wu, T. Wang, B. Lu, X. D. Xu, S. X. Cheng, X. J. Jiang, X. Z. Zhang and R. X. Zhuo, *Langmuir*, 2008, **24**, 10306-10312.
45. D. Y. Teng, Z. M. Wu, X. G. Zhang, Y. X. Wang, C. Zheng, Z. Wang and C. X. Li, *Polymer*, 2010, **51**, 639-646.
46. P. J. Skrzyszewska, F. A. de Wolf, M. W. T. Werten, A. P. H. A. Moers, M. A. C. Stuart and J. van der Gucht, *Soft Matter*, 2009, **5**, 2057-2062.
47. B. Holt, A. Tripathi and J. Morgan, *J. Biomech.*, 2008, **41**, 2689-2695.
48. N. M. Franson and N. A. Peppas, *J. Appl. Polym. Sci.*, 1983, **28**, 1299-1310.
49. D. Ma, K. Tu and L. M. Zhang, *Biomacromolecules*, 2010, **11**, 2204-2212.
50. P. L. Ritger and N. A. Peppas, *J. Controlled Release*, 1987, **5**, 37-42.
51. S. W. Kim, Y. H. Bae and T. Okano, *Pharm. Res.*, 1992, **9**, 283-290.

Graphical Abstract



Novel acid-cleavable and injectable supramolecular hydrogels based on the inclusion complexes between the acid-cleavable star copolymer (mPEG-*a*-PCL-*a*-)₃ and α -CD were prepared, and used as controlled drug delivery depots.